The Astrophysical Journal Letters, 940:L3 (7pp), 2022 November 20 https://doi.org/10.3847/2041-8213/ac9ccf

The Dark Matter Tidal Stripping History of the Sagittarius Core with *N*-body Simulations

Hai-Feng Wang[1], Francois Hammer[1], Yan-Bin Yang[1], and Jian-Ling Wang[2]
[1] GEPI, Observatoire de Paris, Université PSL, CNRS, Place Jules Janssen F-92195, Meudon, France; haifeng.wang@obspm.fr, francois.hammer@obspm.fr, yanbin.yang@obspm.fr
[2] CAS Key Laboratory of Optical Astronomy, National Astronomical Observatories, Beijing 100101, People's Republic of China
Received 2022 June 2; revised 2022 October 19; accepted 2022 October 24; published 2022 November 14

Abstract

The infall of the Sagittarius (Sgr) dwarf spheroidal galaxy in the Milky Way halo is an unique opportunity to understand how the different components of a dwarf galaxy could be tidally removed. In this work, we reconstruct the Sgr core morphology and kinematics on the basis of a model that has already successfully reproduced the Sgr stream. Here we use a very high resolution model that almost resolves individual stars in the Sgr core. It reproduces most of the observed morphology and kinematic properties, without specific fine tuning. We also show that the dark matter may have been almost entirely stripped by Milky Way tides after two passages at the pericenter. Finally the model predicts that the Sgr core will be fully disrupted within the next 2 Gyr.

Unified Astronomy Thesaurus concepts: Sagittarius dwarf spheroidal galaxy (1423); Milky Way disk (1050)

1. Introduction

Our understanding of the formation and evolution of massive galaxies has been limited for a while by the question of disk formation (White & Rees 1978; Navarro et al. 1995). This has substantially progressed in the last decade by the discovery that many massive galactic disks are rejuvenated by major mergers (Hammer et al. 2005, 2009; Robertson & Bullock 2008; Stewart et al. 2009). However, the formation and evolution of dwarf galaxies is still a matter of debate. For example, the proximity of Milky Way (MW) dwarfs to their pericenters (Simon 2019; Hammer et al. 2020) may question their dark matter content. Dwarf galaxies may reveal important properties of their matter content when they are observed in a merging process such as that experienced by the Sgr dwarf galaxy. Since this ongoing minor merger event was discovered by Ibata et al. (1994), a Sagittarius core or remnant has been investigated by many studies (Ibata et al. 1995; Lokas et al. 2010; Penarrubia et al. 2010; Vasiliev & Belokurov 2020; del Pino et al. 2021; Vasiliev et al. 2021). This dwarf galaxy may help to probe the Milky Way potential and may have affected the Milky Way disk (Antoja et al. 2018; Laporte et al. 2018, 2019, 2020; Wang et al. 2018a, 2018b, 2019, 2020a, 2020b, 2020c; López-Corredoira et al. 2020; Yu et al. 2021; Bland-Hawthorn & Tepper-Garcia 2021; Yang et al. 2022). There are also globular clusters associated to the Sgr system such as M 54, Ter 8, Ter 7, Arp 2 inside or near the main body of the Sagittarius dwarf spheroidal galaxy, and Pal 12, and Whiting 1 that belong to the trailing arm (Bellazzini et al. 2020).

Using *N*-body simulations under the framework of a tidal stripping scenario, Lokas et al. (2010) presented the first model for the evolution of the Sgr dwarf considering the observed elliptical shape, and suggested that the total mass nowadays within 5 kpc is $5.2 \times 10^8\ M_\odot$ with small intrinsic rotation left. Del Pino et al. (2021) showed that the Sgr core has an S-shape morphology and shows a mild rotation. This has been done on the basis of a machine-learning method for Gaia DR2 RR Lyrae stars and of an *N*-body model whose progenitor is a flattened rotating disk. However, the model is based on a Sgr-like dwarf and a relatively massive Milky Way, which could be quite different from the real Sgr orbiting around the real Milky Way.

Many properties of the Sgr remnant or core are still under debate, e.g., the Sgr core mass and its dynamical state, which is likely affected by MW tides. Vasiliev & Belokurov (2020) showed that a tidally disrupted Sgr making 2.5 orbits around the Milky Way could reproduce well the core observational properties, for which they found a present-day core mass of $4.0 \times 10^8\ M_\odot$ within a 5 kpc radius. Recently, Wang et al. (2022) considered a Milky Way mass of $5.2 \times 10^{11}\ M_\odot$ and an initial Sgr mass of $9.3 \times 10^8\ M_\odot$ with a similar initial orbit than that used by Vasiliev et al. (2021) and for which they assumed a total MW mass of $9 \times 10^{11}\ M_\odot$. To retrieve the Sgr stream, Wang et al. (2022) have scaled down many mass properties of Vasiliev & Belokurov (2020) and Vasiliev et al. (2021), and have adopted a rotating disk for the Sgr progenitor, together with a dark matter scale length of 1.6 kpc.

They have also been able to reproduce as well 3D spatial features of the Sgr stream, including its leading and trailing arms. Moreover and conversely to the Vasiliev & Belokurov (2020) model, the Wang et al. (2022) model is able to reproduce the observed north and south bifurcations, which were first discovered in Belokurov et al. (2006) and Koposov et al. (2012), respectively (see also Oria et al. 2022).

Here we follow the Wang et al. (2022) study, using a much higher resolution version of their model, in order to generate the detailed Sgr core physics, including kinematics, and the way stars and dark matter have been stripped.

This Letter is structured as it follows. In Section 2, we focus on the modeling details. In Section 3 we discuss how the core properties are reproduced, and we also show the dark matter stripping history, then we show the stellar or dark matter distribution at the present time. The last Section includes the discussion and then the conclusions.

Table 1
Initial Condition Parameters in This High Resolution Dynamical Simulation

Parameter	Milky Way	Sagittarius	Units
Particle mass (star/dark matter)	1.375 (5.575) × 10^5	13.75(55.13)	$M_\odot$
Dark matter mass	4.8 × 10^{11}	9.0 × 10^8	$M_\odot$
Dark matter scale	9.1	1.6	kpc
Stellar disk mass	3.58 × 10^{10}	3.0 × 10^7	$M_\odot$
Stellar scale length	2.4	0.3	kpc
Stellar scale height	0.24	0.15	kpc
Bulge mass	1.12 × 10^{10}	N/A	$M_\odot$
Bulge scale	0.4	N/A	kpc
Number of particle	1.2	18	Million
Initial position		(66, −9, 27)	kpc
Initial velocity		(−48, −17, 65)	km s^{-1}

2. Modeling Parameters

Here we give a concise review of our high resolution modeling for which the mass resolution for a dwarf galaxy is 100 times better than the fiducial model in Wang et al. (2022), i.e., 13.75 solar mass per Sgr particle instead of 1375 solar mass. The Milky Way model has been constructed following Barnes (2002), and it includes a bulge, an exponential stellar disk, and a core dark matter halo, while the Sgr dwarf galaxy is made of a dark matter halo and of a disk (see Table 1). The halo density profile is converging at large radii. More details about the modeling components could be found in Barnes (2002) and in Wang et al. (2022). The modeling is realized using GIZMO (Hopkins 2015) and Table 1 gives the initial conditions. In order to avoid numerical/artificial kick between heavy MW particles and light dwarf galaxy particles, the technique of adaptive gravity softening (Hopkins et al. 2018) has been adopted. The minimal softening is set to 2.5 pc (e.g., for interactions between light particles), which allows a full resolution of dynamics within the core scale length (300 pc) of Sgr dwarf galaxy.

However, the adaptive softening is not a magic fix for having very different particle masses (see Table 1). We have first verified the absence of anomalous motions especially during the pericenter passages. Second, we have replaced the Milky Way (bulge, disk, and halo) particles by an analytic potential having precisely the same initial parameters (sizes and masses), and have verified whether the velocity dispersion of stars has been affected by numerical heating. The latter is detected only during the short-timescale passages to the pericenter, after which values of our model cannot be distinguished from that of the analytic potential. Third, we have run a simulation with a higher resolution, in which the mass of MW particles has been divided by 10. We retrieve the same results, i.e., numerical heating mildly affects stellar velocity for a short time, during pericenter passages. We then conclude that our simulations can be well representative of the Sgr core kinematics and morphology (see Appendix).

In this work the core/stream is projected in right-hand Galactocentric Cartesian coordinates (van der Marel et al. 2002; [X, Y, and Z]). We have adopted the solar motion from Drimmel & Poggio (2018) with $[U_\odot\ V_\odot\ W_\odot] = [12.9, 12.6, 7.78]$ km s^{-1}. The circular speed of the local standard of rest is adopted to be 233 km s^{-1} (Drimmel & Poggio 2018). The distance of the Sun from the Galactic center is chosen to be $R_\odot = 8.277$ kpc (GRAVITY Collaboration et al. 2022) and $Z_\odot = 20.8$pc (Bennett & Bovy 2019), and we have verified that different solar motions and coordinates would not change our final conclusions. We have also verified that our models remain stable when evolved in isolation for several Gyr.

3. Results

Figure 1 shows the 3D stellar density and 3D kinematic distributions of the Sgr core for both modeling (left panels) and observations (right panels) from del Pino et al. (2021) (see their Figure 10). The top panels reveal the S-shape in the x–z plane, which is surrounded by star motions indicated by black arrows that indicate stellar motions (v_x, v_z) after subtraction of the center of mass (COM) velocity. It suggests that tidal stripping becomes prominent at 2 kpc from the Sgr center, where the stars of the Sgr core are progressively removed from the main body to feed the stream. By accounting for this mechanism, the simulations reproduce well the observed morphology and kinematics of the Sgr core in the x–z plane. Similarly, simulations shown in the middle left panel (x–y plane) present an almost circular shape as it is observed, as well as a relatively chaotic distribution of velocities shown as black arrows based on v_x, v_y. Black arrows in the z–y plane indicate an expansion of the stars in the outskirts of the core for both data and modeling (see bottom panels). Besides this, in the z–y plane the morphology of the modeled Sgr core appears to be more elongated than the observed one.

We also note that the S-shape is caused by the later tidal disruption and it is not a long lived structure. A more detailed map of the Sgr core stellar motions is given in the Appendix.

In Figure 1 the large blue arrow shows the projection of the internal angular momentum, for which a good agreement is found between observations and modeling, except perhaps in the x–z plane (top panel) for which their orientations differ by ∼30 degrees. The large orange arrow represents the COM velocity direction, for which observations and modeling agrees within 5 degrees. In the x–z and y–z planes the core shows a counterclockwise and clockwise rotation, respectively. It appears that the model reproducing well the whole Sgr stream compares quite well with the observations of the Sgr core of del Pino et al. (2021) for both morphology and kinematics. However the dynamics, and in particular for the internal angular momentum direction, is not fully recovered, and to reach a perfect matching between modeling and observations would require some further fine tuning.

However, we think that the most important change to be done would be to introduce the gas in the Sgr progenitor, since it is likely a gas-rich irregular dwarf. Gas stripping history was revealed by Tepper-Garcia & Bland-Hawthorn (2018), showing that the gas has been lost about 1 Gyr ago. If adding gas could not improve the modeling, one may consider increasing the number of parameters, e.g., by adding an extra massive LMC or considering a non-spherical Milky Way halo, for example, Vasiliev et al. (2021) have added a massive LMC and a twisted halo, which helped them in reproducing the Sgr stream.

Our modeling suggests a current Sgr core deficient in dark matter as it is shown in Figure 2, which gives the time evolution of both dark and stellar matter within a radius of 5 kpc (top panels) and 2 kpc (bottom panels). The left panels show the evolution of the dark matter/stellar mass ratio that varies from an initial value of 20 (13 in the bottom panel) to almost zero after 4.7 Gyr evolution. During the same elapsed

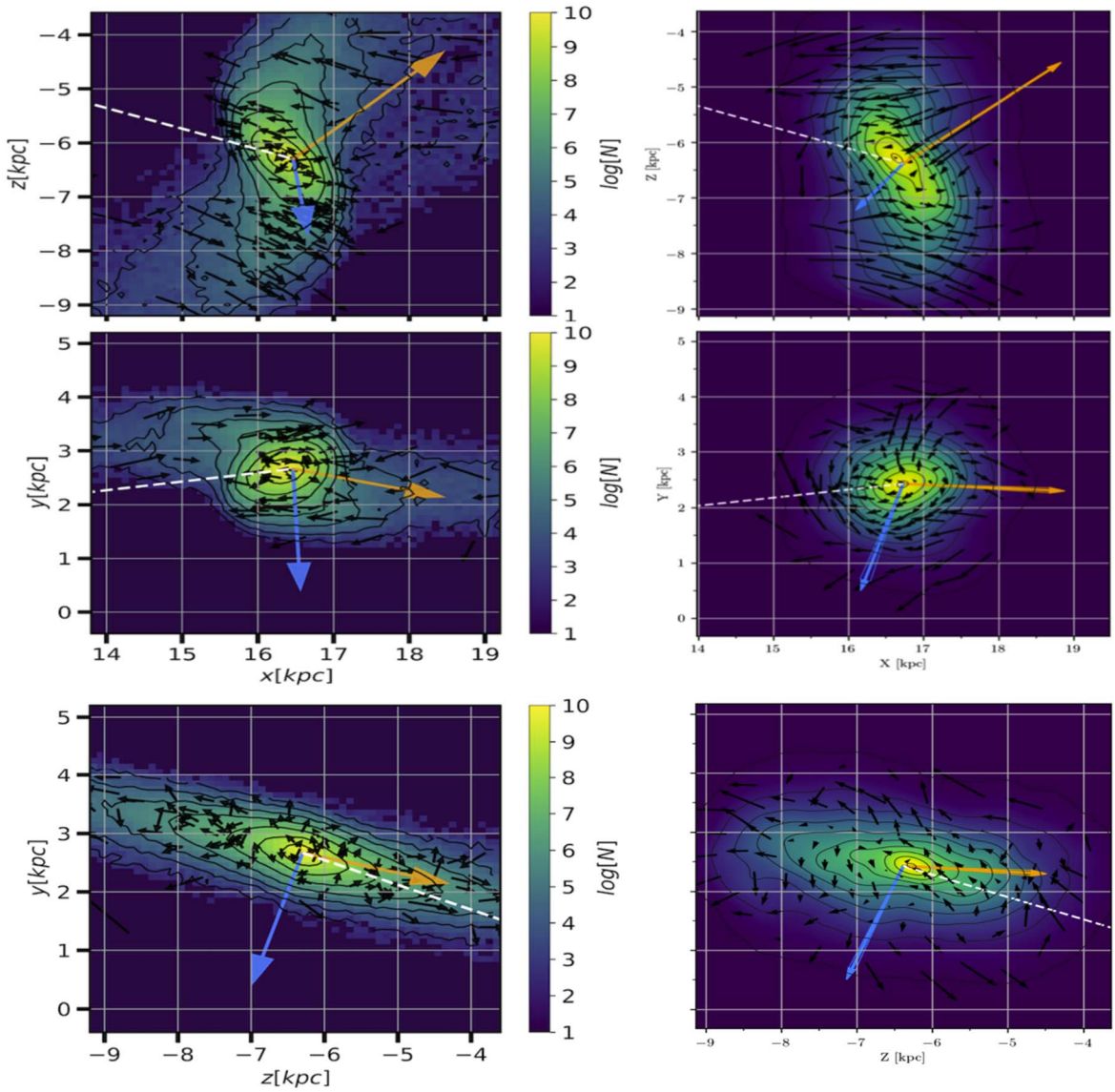

Figure 1. Left column: Sgr core density and kinematics of the model projected on the Galactocentric x–z, x–y, and z–y planes. Stellar density is shown by black contours and colored from yellow to blue. The projected tangential velocities after subtraction of the COM velocity are shown by the black arrows and the orange arrows indicate the projected bulk velocity of the COM region. The blue arrow shows the projection of the internal angular momentum. The direction toward the MW center is indicated by the white dashed line. All arrows are scaled in order to be clearly shown for physical discussion. Right column: the observational results from Pino et al. (2021) (see their Figure 10) that are shown for comparison. A more detailed view of the stellar motions is shown in the Appendix in Figure 5.

time, the stellar mass decreases from 3×10^7 $M_\odot$ to 1.4 (1.1) $\times 10^7$ $M_\odot$, corresponding to a mass-loss rate of 53% (63%) as seen in the middle panel of Figure 2. This stellar mass loss contrasts with that of the dark matter, for which the mass is decreasing from 6 (4) $\times 10^8$ $M_\odot$ to almost zero according to the right panels of Figure 2. In other words, almost all the dark matter content of Sgr has been lost from its core, and Sgr becomes almost dark matter free at the present epoch.

We also note that the model of Vasiliev & Belokurov (2020) leads to a smaller elapsed time for the Sgr disruption, while also fitting the stream very well. This mainly comes from their MW model that is more massive than ours, leading to larger gravitational forces and then shorter times. Other differences are due to different choices in implementing the Sgr progenitor (e.g., a disk or a spheroid, and initial abundance of dark matter).

Moreover, it appears that dark matter losses occurred mostly during pericenter passages, which sufficed to almost fully empty it 3 Gyr ago. Dark matter studies of dwarf galaxies have often excluded Sgr because of its strong interaction with the Milky Way. Such guesses are robustly confirmed by our study that suggests a dark matter deficient Sgr core, for which most properties are led by the Milky Way tidal forces.

Figure 3 shows the leading, trailing, north and south bifurcation of the Sgr stellar stream in the (X, Z) plane. It also evidences how the distribution of dark matter particles (bottom panel) differs from that of the stars forming the Sgr stream (top panel). This illustrates well that dark matter populating the galactic halo does not interact through gravitational torques and lets the stream be almost only populated by stars.

4. Discussion and Conclusions

In their modeling Vasiliev & Belokurov (2020) found a remnant stellar mass within a 5 kpc radius of 10^8 $M_\odot$ assuming

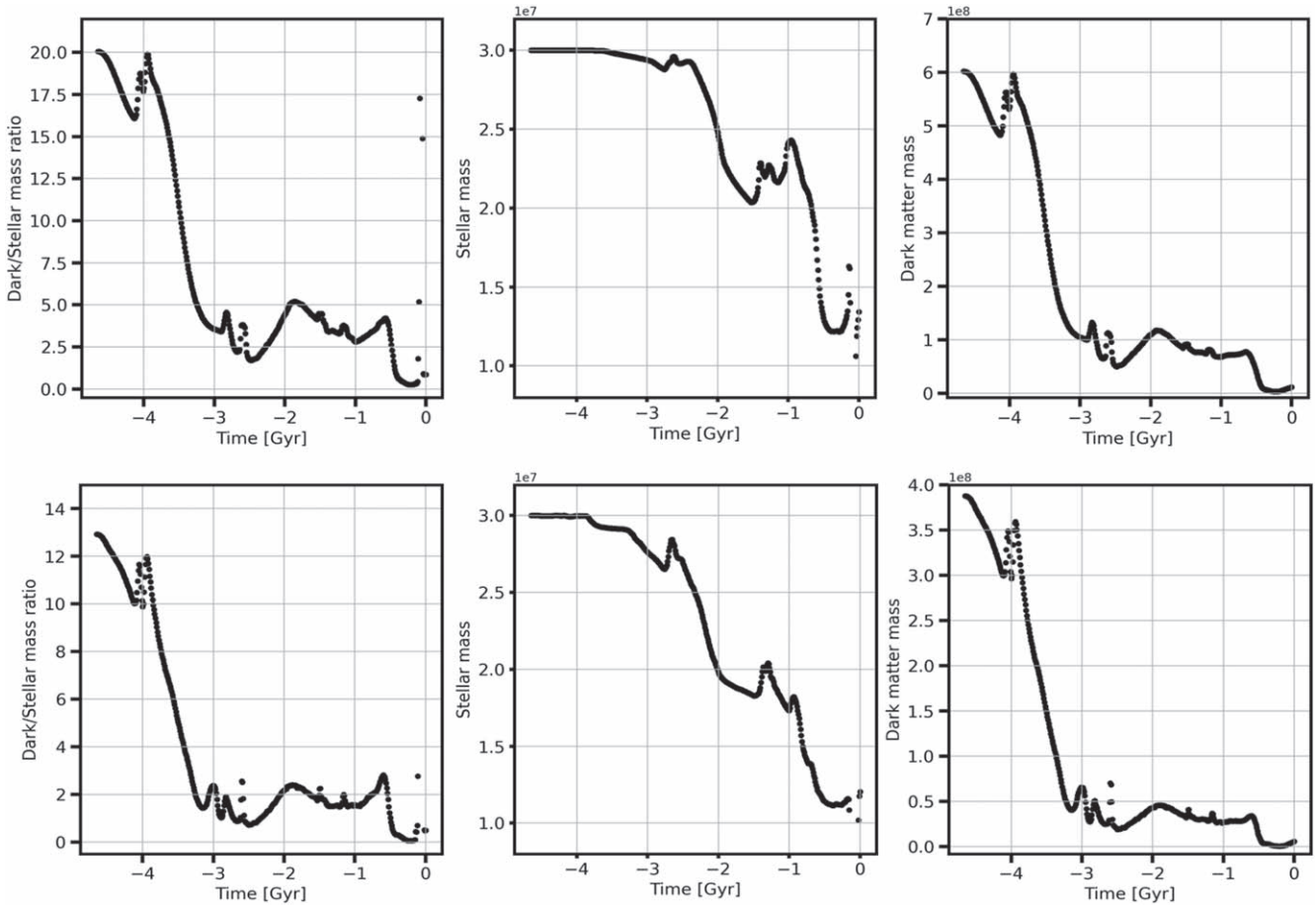

Figure 2. It shows the dark matter and stellar mass evolution history during our simulation over a 4.7 Gyr duration (top panels: within a radius of 5 kpc; bottom panels: within a 2 kpc radius). The left, middle, and right panels show the ratio of dark matter to the stellar mass, the stellar stripping history of the core, and that of the dark matter.

few kiloparsecs for the dark matter scale radius. In this work we give the evolution history of both dark matter and stellar masses within 2 or 5 kpc in Figure 2 while the initial dark matter scale length is 1.6 kpc. This contrasts with our finding of only $1.4 \times 10^7\ M_\odot$ within the same radius. Determining the stellar mass of the Sgr core is not a simple exercise, because (i) it lies near the MW disk leading to severe extinction and confusion effects, and (ii) the core limits are not easy to determine as it is directly linked to the stream (see Figure 1) as expected from the Sgr tidally disrupted nature. For example, Majewski et al. (2003) (see also Simon 2019) found that Sgr has a V-band luminosity of $2.1 \times 10^7\ L_\odot$, which contrasts with the much larger value found by Niederste-Ostholt et al. (2010), who made an intensive stellar count study and find around 10 $(9.6-13.2) \times 10^7\ L_\odot$ for which 30% is associated to the the Sgr core and 70% to the stream. Assuming a factor 1.5 for converting luminosity into stellar mass for a galaxy containing intermediate-age stars, one can find $3 \times 10^7\ M_\odot$ from Simon (2019), and $4.5 \times 10^7\ M_\odot$ for the core mass of Sgr from Niederste-Ostholt et al. (2010), which is likely an upper limit since their estimates include stars lying up to 10 kpc (see their Figure 9) instead of the 5 kpc radius adopted by Vasiliev & Belokurov (2020). Given the above observational limits, it means that the core mass ($10^8\ M_\odot$) recovered from the model of Vasiliev & Belokurov (2020) may overestimate while this Letter ($1.4 \times 10^7\ M_\odot$) may underestimate the core stellar mass by a factor between 2 to 3, respectively. Perhaps more important for our modeling is the good agreement that predicts the correct fraction of stars in the stream and in the core (see Figure 2).

In summary, the model presented by Wang et al. (2022) that reproduces the Sgr stream including its bifurcation behavior is also able to successfully reproduce most of the Sgr core properties as it is shown in this work. Without specific fine tuning, the modeling reproduces most of the core morphology, including the S-shape, as well as most of its kinematics, including the tidally removed stars at its S-shape edges, which are forming the Sgr stream. We are however aware that there are some discrepancies between the modeling and the observations, and these are mostly linked to the internal angular momentum poles, which may suggest to investigate an initially gas-rich Sgr.

As another result, this study shows how stars and dark matter are tidally removed from the core, the dark matter being almost completely stripped as it is expected from theory. This model also predicts that the Sgr core will disappear within 2 Gyr, leaving only its central cluster intact.[3]

The authors gratefully acknowledge the support of K.C. Wong Education Foundation. We appreciate the support of

[3] This can be seen in a video showing the evolution of star particles as shown in the top of Figure 3: https://youtu.be/EqjEQpWaeIU.

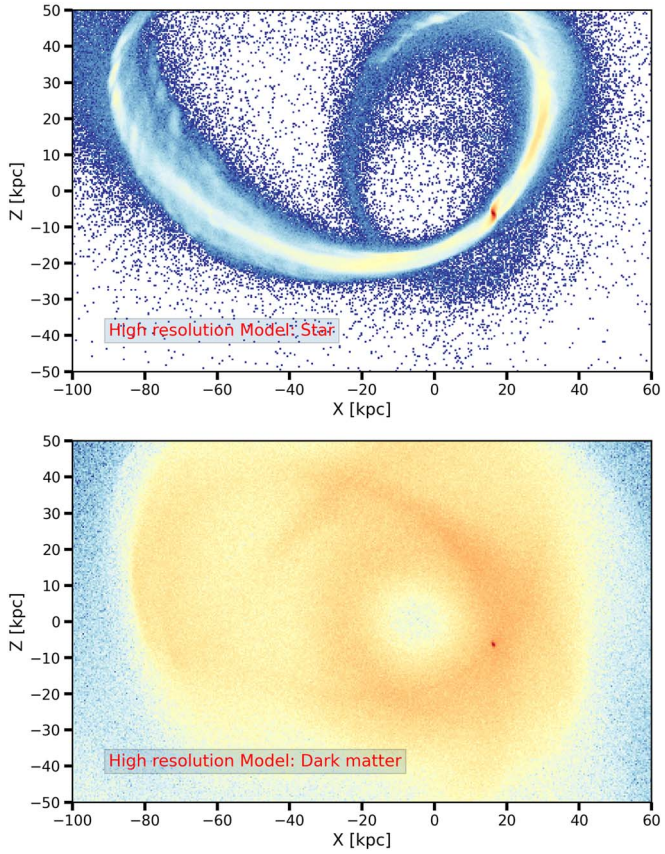

Figure 3. It shows stellar and dark matter tracks at the present time after 4.7 Gyr evolution. The top panel shows the stellar leading, trailing arm, core, north and south bifurcation. The bottom panel indicates how the dark matter may distribute differently than stars.

the International Research Program Tianguan, which is an agreement between the CNRS in France, NAOC, IHEP, and the Yunnan University in China. Y.Y. thanks the National Natural Foundation of China (NSFC No. 11973042). Simulations in this work were performed at the High-performent calculation (HPC) resources MesoPSL financed by the project Equip@Meso (reference ANR-10-EQPX-29-01) of the program "Investissements d'Avenir" supervised by the 'Agence Nationale de la Recherche'. We are very grateful to Gary Mamon, Eugene Vasiliev, Frederic Arenou, Carine Babusiaux, Piercarlo Bonifacio, Jiang Chang, Yongjun Jiao, and Marcel Pawlowski for the numerous and illuminating discussions we have had on the Sgr simulation. We thank the referee for giving us precious advice and suggestions that have seriously improved the manuscript. H.F.W. acknowledges the science research grants from the China Manned Space Project with No. CMS-CSST-2021-B03. We are grateful to Phil Hopkins who kindly shared with us the access to the Gizmo code.

Data Availability: The data underlying this article will be shared on reasonable request to the corresponding author.

Appendix
More comparisons and Investigations

This part is about more comparisons and investigations for core kinematics and numerical heating. Figure 4 confirms that the artificial kicking happens only for short durations near the pericenter passage, and has a marginal impact to the results and conclusions of the paper. Figure 5 presents a more detailed view of the stellar motions of the core.

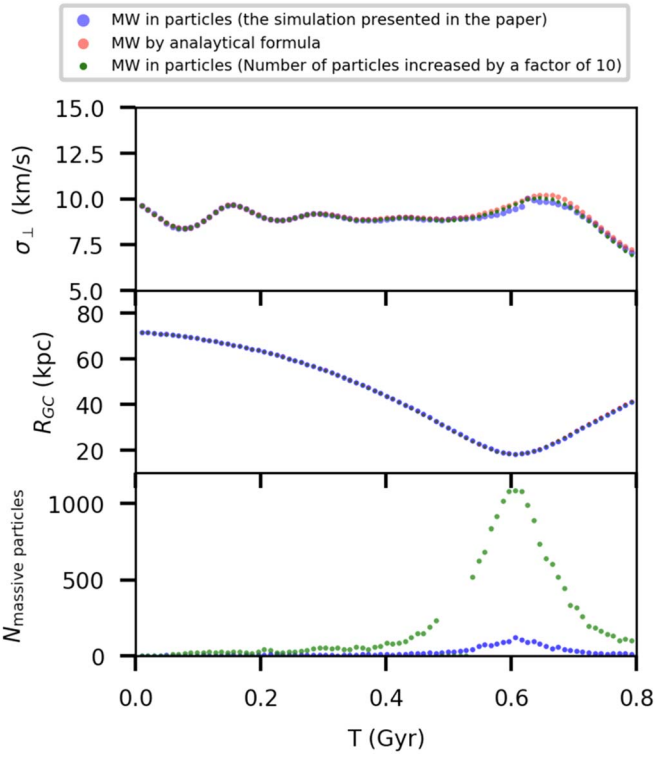

Figure 4. It compares our full-particle simulation presented in the Letter and this simulation with the analytical MW (see the blue and red dots, respectively). The latter is assumed without numerical heating, since it does not possess massive particles. From top to bottom: the velocity dispersion perpendicular to the orbital plane, as it is a quantity that could be only affected by the Sgr disk particle motions; the distance of a dwarf galaxy from the MW center; the number of massive MW particles within the Sgr core (with a radius of 2 kpc). For a double check, we ran a new simulation by increasing the resolution of the MW by a factor of 10; see the green dots. It shows a very smooth evolution in the velocity dispersion perpendicular to the orbital plane of a dwarf galaxy, which verifies the concern that using less massive MW particles reduces the artificial kicking. These tests confirm that the artificial kicking happens only for short durations near the pericenter passage, and has a marginal impact to the results and conclusions of the Letter.

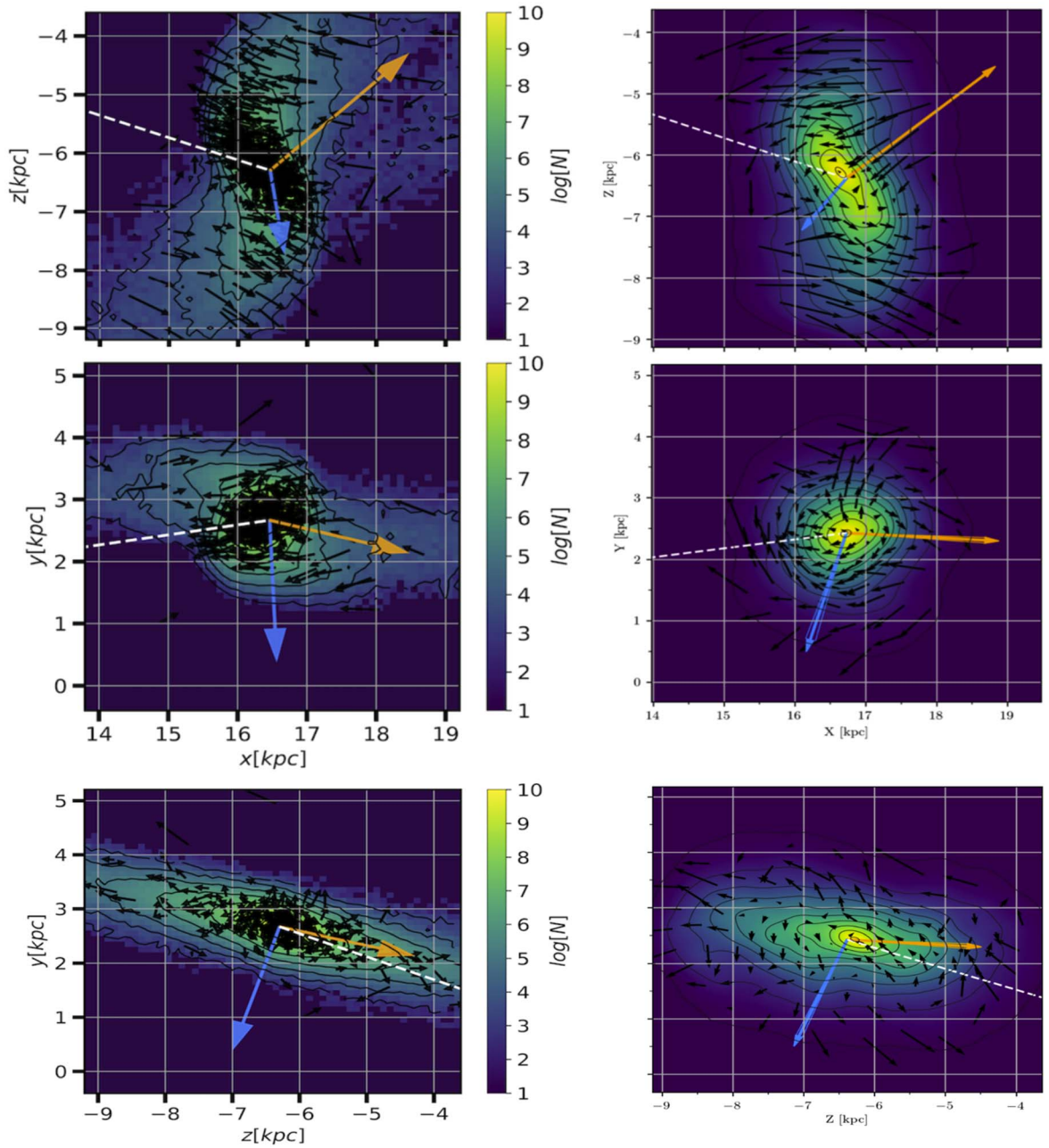

Figure 5. Similar to Figure 1, but with more arrows and points to make the rotation and expansion in the outskirts clearer. Left column: Sgr core density and kinematics of the model projected on the Galactic centric *x*–*z*, *x*–*y*, and *z*–*y* planes. Right column: the observational results from del Pino et al. (2021) (see their Figure 10) that are shown for more comparison.

ORCID iDs

Hai-Feng Wang https://orcid.org/0000-0001-8459-1036
Francois Hammer https://orcid.org/0000-0002-2165-5044

References

Antoja, T., Helmi, A., Romero-Gómez, M., et al. 2018, Natur, 561, 360
Barnes, J. E. 2002, MNRAS, 333, 481
Bellazzini, M., Ibata, R., Malhan, K., et al. 2020, A&A, 636, A107
Belokurov, V., Zucker, D. B., Evans, N. W., et al. 2006, ApJL, 642, L137
Bennett, M., & Bovy, J. 2019, MNRAS, 482, 1417
Bland-Hawthorn, J., & Tepper-García, T. 2021, MNRAS, 504, 3168
del Pino, A., Fardal, M. A., van der Marel, R. P., et al. 2021, ApJ, 908, 244
Drimmel, R., & Poggio, E. 2018, RNAAS, 2, 210
GRAVITY Collaboration, Abuter, R., Aimar, N., Amorim, A., et al. 2022, A&A, 657, L12
Hammer, F., Flores, H., Elbaz, D., et al. 2005, A&A, 430, 115
Hammer, F., Flores, H., Puech, M., et al. 2009, A&A, 507, 1313
Hammer, F., Yang, Y., Arenou, F., et al. 2020, ApJ, 892, 3
Hopkins, P. F. 2015, MNRAS, 450, 53
Hopkins, P. F., Wetzel, A., Kereš, D., et al. 2018, MNRAS, 480, 800
Ibata, R. A., Gilmore, G., & Irwin, M. J. 1994, Natur, 370, 194
Ibata, R. A., Gilmore, G., & Irwin, M. J. 1995, MNRAS, 277, 781
Koposov, S. E., Belokurov, V., Evans, N. W., et al. 2012, ApJ, 750, 80
Laporte, C. F. P., Belokurov, V., Koposov, S. E., Smith, M. C., & Hill, V. 2020, MNRAS, 492, L61
Laporte, C. F. P., Johnston, K. V., Gómez, F. A., Garavito-Camargo, N., & Besla, G. 2018, MNRAS, 481, 286
Laporte, C. F. P., Minchev, I., Johnston, K. V., & Gomez, F. A. 2019, MNRAS, 485, 3134
Lokas, E. L., Kazantzidis, S., Majewski, S. R., et al. 2010, ApJ, 725, 1516

López-Corredoira, M., Garzón, F., Wang, H.-F., et al. 2020, A&A, 634, A66
Majewski, S. R., Skrutskie, M. F., Weinberg, M. D., & Ostheimer, J. C. 2003, ApJ, 599, 1082
Navarro, J. F., Frenk, C. S., & White, S. D. M. 1995, MNRAS, 275, 720
Niederste-Ostholt, M., Belokurov, V., Evans, N. W., & Penarrubia, J. 2010, ApJ, 712, 516
Oria, P.-A., Ibata, R., Ramos, P., Famaey, B., & Errani, R. 2022, ApJL, 932, L14
Penarrubia, J., Belokurov, V., Evans, N. W., et al. 2010, MNRAS, 408, L26
Robertson, B. E., & Bullock, J. S. 2008, ApJL, 685, L27
Simon, J. D. 2019, ARA&A, 57, 375
Stewart, K. R., Bullock, J. S., Wechsler, R. H., et al. 2009, ApJ, 702, 307
Tepper-García, T., & Bland-Hawthorn, J. 2018, MNRAS, 478, 5263
van der Marel, R. P., Alves, D. R., Hardy, E., & Suntzeff, N. B. 2002, AJ, 124, 2639
Vasiliev, E., & Belokurov, V. 2020, MNRAS, 497, 4162, (VB20)
Vasiliev, E., Belokurov, V., & Erkal, D. 2021, MNRAS, 501, 2279
Wang, H.-F., Carlin, J. L., Huang, Y., et al. 2019, ApJ, 884, 135
Wang, H. F., Huang, Y., Zhang, H.-W., et al. 2020a, ApJ, 902, 70
Wang, H. F., Liu, C., Xu, Y., et al. 2018a, MNRAS, 478, 3367
Wang, H. F., López-Corredoira, M., Carlin, J. L., et al. 2018b, MNRAS, 477, 2858
Wang, H. F., López-Corredoira, M., Huang, Y., et al. 2020b, MNRAS, 491, 2104
Wang, H. F., López-Corredoira, M., Huang, Y., et al. 2020c, ApJ, 897, 119
Wang, H. F., Yang, Y. B., Hammer, F., et al. 2022, arXiv:2204.08542
White, S. D. M., & Rees, M. J. 1978, MNRAS, 183, 341
Yang, P., Wang, H.-F., Luo, Z.-Q., et al. 2022, arXiv:2205.09227
Yu, Y., Wang, H.-F., Cui, W.-Y., et al. 2021, ApJ, 922, 80